Trans Indian Inst Met (2019) 72(3):581–589
https://doi.org/10.1007/s12666-018-1456-z

TECHNICAL PAPER

Reducing the Sintering Flue Gas Pollutants Emissions Based on the Accumulation Heat Effect in Iron Ore Sintering Process

J. M. Qie[1,2] · C. X. Zhang[1] · Y. H. Guo[1] · H. F. Wang[1] · S. L. Wu[2]

Received: 19 August 2018 / Accepted: 4 November 2018 / Published online: 25 January 2019

Abstract The pressure to reduce the emissions of the flue gas pollutants from iron ore sintering is enlarging increasingly. Based on the accumulation heat effect of sinter bed, the reasonable distribution of fuel in sinter bed was identified through the calculation of material balance and heat balance of raw materials. The sinter bed with a height of 300 mm was divided into three units, and the average available accumulation heat rate was about 38%. The reasonable coke powder addition ratio of each unit was 6.6%, 5.7%, and 5.2%, respectively, from the top to the bottom of sinter pot. The sinter-pot test results showed that the fuel consumption and the emissions of SO_2, NO_x, CO, and CO_2 was reduced by 7.5 kg/t, 57.7%, 18.4%, 72.5%, and 31.7%, respectively, when compared with the conventional method in which the coke powder addition ratio of raw materials was 6.6%. Meanwhile, the sinter quality was improved.

Keywords Iron ore sintering · Accumulation heat · SO_2 · NO_x · CO · CO_2

✉ J. M. Qie
907360382@qq.com

[1] State Key Laboratory of Advanced Steel Process and Products, Central Iron and Steel Research Institute, Beijing 100081, People's Republic of China

[2] School of Metallurgical and Ecological Engineering, University of Science and Technology Beijing, Beijing 100083, People's Republic of China

1 Introduction

The energy consumption of iron ore sintering process accounts for 10–15% of the total energy consumption of steel manufacturing process. Meanwhile, the consumption of solid fuel accounts for 75–80% of the energy consumption of iron ore sintering process [1, 2]. Most of SO_2 and about 90% of NO_x are produced by the burning of solid fuel in iron ore sintering process [3, 4]. The emission of SO_2 and NO_x of iron ore sintering process account for 60% and 50% of the total emissions of SO_2 and NO_x of steel manufacturing process, respectively [5, 6]. Meanwhile, carbon emission of iron ore sintering process accounts for more than 20% of the total carbon emission of steel manufacturing process [7].

The accumulation heat effect of sinter bed is the result of the heating action from the upper sintering mixture to the lower sintering mixture and the preheating effect from the upper sintering mixture to the airflow, which passes the lower sintering mixture [8]. The existence of the accumulation heat effect in iron ore sintering process leads to the nonuniform sinter quality along the height of the sinter bed, the decrease in sinter yield, and the large energy consumption [9]. The reasonable distribution of fuel is to reduce the fuel consumption gradually along the height of the sinter bed utilizing the accumulation heat effect, which is helpful in improving the temperature uniformity of sinter bed and sinter quality [10]. Kpchko studied the relationship between the physical heat of sinter and the height of sinter bed [11]. The results showed that the physical heat of sinter increased along the height of the sinter bed. Huang et al. [12] analyzed and calculated the accumulation heat effect of sinter bed and put forward the calculation model for the reasonable distribution of fuel in sinter bed. Bai et al. [13] constructed an accumulation heat effect model of sinter bed

and studied some related influence factors. Xu [2] developed segregation feeding and airflow feeding technology based on the accumulation heat effect of sinter bed. Nippon Steel reduced the fuel consumption by 6.3 kg/t through double-layer sintering [14]. Li et al. [15] optimized the fuel distribution in sinter bed based on the highest temperature control in iron ore sintering process. Zhang et al. [16] analyzed the heat and mass transfer in two-layer sintering process. Huang et al. [17] constructed an optimization model of fuel distribution in sinter bed, and the sinter-pot test results showed that the fuel consumption was reduced by 3.83 kg/t.

Most of the related researches have focused on the reduction in the fuel consumption and the improvement in sinter quality, while ignoring its reduction effect on the iron ore sintering flue gas pollutants. In this paper, through the calculation of material balance and heat balance of raw materials, we have investigated the change in emission of SO_2, NO_x, CO, and CO_2 in iron ore sintering process and sinter quality by reasonable distribution of fuel in sinter bed based on the accumulation heat effect of sinter bed through sinter-pot test.

2 Materials and Experiment Methods

2.1 Raw Materials for Sinter-Pot Test

The chemical compositions and ratios of raw materials for sinter-pot test are shown in Table 1. A part of return fines was chosen as raw material and combined with the actual sintering products.

2.2 The Calculation of the Accumulation Heat Effect in Iron Ore Sintering Process

The study of the accumulation heat effect along the height of sinter bed based on the heat distribution law of sinter bed was the basis of realizing the reasonable distribution of fuel in sinter bed. Meanwhile, the calculation of material balance and heat balance was the basis of the calculation of the accumulation heat effect in iron ore sintering process.

This paper used sinter pot as research object, and the reasonable distribution of fuel in sinter bed was indentified based on the calculation of material balance and heat balance of the above raw materials. It was expected to realize the reduction in the fuel consumption and the emissions of the iron ore sintering flue gas pollutants.

2.3 The Sinter-Pot Test

The sinter-pot test and its operation parameters are shown in Fig. 1. A hearth layer of about 20 mm was placed onto the bottom of sinter pot while putting raw materials into sinter pot. The hearth layer consisted of sinter with a size of $10 \sim 16$ mm. Subsequently, the raw materials were put into the sinter pot. The liquid gas-fired burner operated continuously at 1200 °C for 180 s in order to ignite raw materials. The ignitor was removed from sinter pot after ignition. Meanwhile, the flue gas components were recorded. After the test, the sinter was removed from the sinter pot and a series of tests were conducted. The test included the chemical compositions, tumbler strength, reduction index (RI), softening–melting properties, and so on.

Table 1 Chemical compositions and ratios of raw materials (wt%)

Raw materials	TFe	CaO	SiO_2	MgO	Al_2O_3	LOI	Ratios
A ore	64.9	0.21	2.52	0.21	1.32	2.25	14.5
B ore	59.2	0.12	3.70	0.24	2.12	8.79	7.53
C ore	60.3	0.15	3.75	0.14	1.25	8.75	11.4
D ore	63.2	0.22	6.52	0.25	1.32	1.21	13.4
E ore	62.8	0.21	3.20	0.16	1.25	5.20	14.5
Quicklime	–	76.4	4.65	3.86	1.22	12.4	2.54
Dolomite	–	33.2	3.81	18.73	1.25	42.8	5.34
Limestone	–	50.6	3.35	3.23	1.46	41.2	6.65
Return fines	57.3	8.25	4.64	1.62	1.76	2.58	17.7
Coke powder	6.32	9.02	40.3	1.82	29.2	–	6.60
Industrial analysis for coke powder		Fixed carbon: 82.3%; volatile: 3.60%; ash: 14.1%					

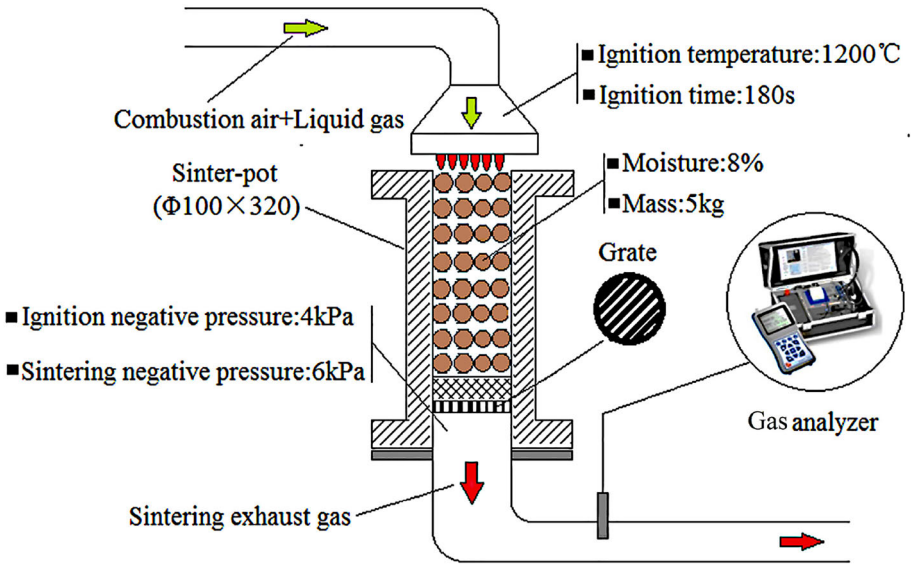

Fig. 1 Diagram of sinter-pot test

3 The Calculation Process and its Results of the Accumulation Heat Effect

We have investigated and calculated the accumulation heat capacity along the height of sinter bed based on the above raw materials in order to achieve a reasonable distribution of fuel in sinter bed.

3.1 The Calculation Process of the Accumulation Heat Capacity of Sinter Bed

Taking sinter-pot ($\Phi 100 \times 320$) as a research object, the height of sinter bed is 300 mm and the hearth layer is 20 mm. The sinter bed is divided into three equal parts along the height (Fig. 2). Each part of sinter bed ($\Phi 100 \times 100$) has been identified as a calculation unit.

The calculation of material balance and heat balance is the basis of the calculation of accumulation heat capacity of sinter bed. The calculation of the accumulation heat capacity mainly focuses on incoming heat and heat output in iron ore sintering process (Fig. 3). The incoming heat includes ignition heat, sintering process heat, and the heat that come from the flue gas in the upper units and is transferred to the succeeding units. The heat output includes sintering process heat consumption, the physical heat of sinter, heat loss, and the heat of the flue gas in this unit transferred to the succeeding units.

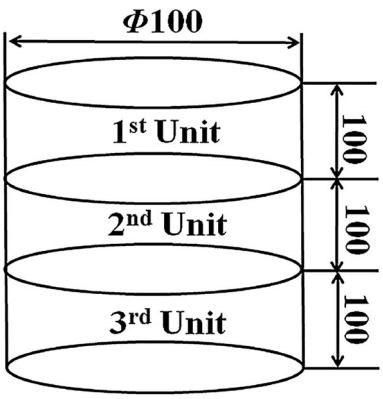

Fig. 2 Diagram of the calculation unit

The ignition heat only affects the first unit, and the effect of other heat input is equivalant to three calculation units. 70% of heat that comes from the flue gas in the first unit becomes a part of heat input for the second unit. 30% of heat that comes from the flue gas in the first unit and 70% of heat that comes from the flue gas in the second unit become a part of incoming heat for the third unit [18].

(1) The physical heat of sinter

The relationship between the temperature of sinter bed and its height is as follows [19]:

$$y = -0.0019x^2 + 4.125x - 300,$$

The calculation formula of the physical heat of sinter is as follows:

$$Q_{\text{sinter}} = \left(G + G_{\text{f}} + G_{\text{p}}\right) \times C_{\text{sb}} \times t_{\text{sk}},$$

where y is the temperature of sinter bed, °C; x is the height from the raw material layer to the sinter layer, $x \geq 100$ mm; G is the mass of sinter whose volume is 7.85×10^{-4} m^3, kg; G_{f} is the mass of return fines, kg; G_{p} is the mass of hearth layer, kg; C_{sb} is the specific heat capacity of sinter, kJ/(kg K); t_{sk} is the temperature of the unit sinter, °C.

(2) The total accumulation heat rate (η_{tol}, %)

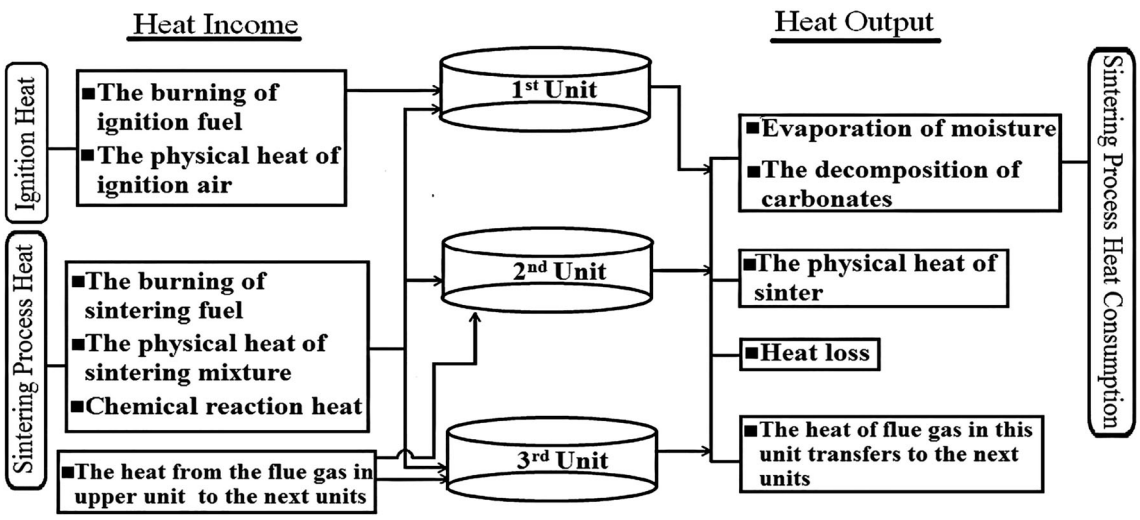

Fig. 3 Components of the calculation of the accumulation heat capacity

The total accumulation heat rate (η_{tol}, %) refers to the ratio of the accumulation heat that comes from the flue gas in the upper units and is transferred to this unit to the total incoming heat of the unit, without taking into account the physical heat of sinter.

The calculation formula of the η_{tol} is as follows:

$$\eta_{\text{tol}} = Q_1/Q_0 \times 100\%,$$

where η_{tol} is the total accumulation heat rate, %; Q_1 is the heat that comes from the flue gas in the upper units and is transferred to this unit, MJ; Q_0 is the total incoming heat of this unit, MJ.

(3) The available accumulation heat rate (η_{avl}, %)

The available accumulation heat rate (η_{avl}, %) refers to the ratio of the available accumulation heat of the unit to the total incoming heat of the unit. The available accumulation heat equals to the heat that comes from the flue gas in the upper units and is transferred to this unit minus the physical heat of sinter of this unit. The η_{avl} is more useful than the η_{tol} as the physical heat of sinter is unavailable at the end of sintering.

The calculation formula of the η_{avl} is as follows:

$$\eta_{\text{avl}} = (Q_1 - Q_s)/Q_0 \times 100\%,$$

where η_{avl} is the available accumulation heat rate of the unit, %; Q_{S} is the physical heat of sinter of this unit, MJ.

(4) The coke powder addition of each unit

The coke powder addition of each unit equals the original coke powder addition of each unit minus the reduction in coke powder as a result of the accumulation of heat.

The calculation formula of the coke powder addition of each unit is as follows:

$$G' = G_0 - Q_{\text{ayl}}/q,$$

where G' is the coke powder addition per ton of dry raw materials of the unit, kg/t; G_0 is the original coke powder addition per ton of dry raw materials of the unit, kg/t; Q_{ayl} is the available accumulation heat per ton of dry raw materials of the unit, MJ/t; q is the calorific value of per unit mass of coke, kJ/g.

3.2 The Calculation Results of the Accumulation Heat Capacity of Sinter Bed

In the calculation results of heat balance (Fig. 4), the accumulation heat ratio and the coke powder addition of each unit (Table 2) are based on the calculation of material balance and heat balance of raw materials while adding 6.6% coke powder. The heat coming from the flue gas in the upper unit increases from 1329.4 kJ in the second unit to 1967.8 kJ in the third unit. The ratio of heat that come from the flue gas in the upper unit to the total incoming heat of the unit increases from 33% in the second unit to 42% in the third unit. The accumulation heat effect increases gradually. The heat of the flue gas in this unit that is transferred to the succeeding units reduces from 1899.1 kJ in the first unit to 1201.5 kJ in the third unit. The ratio of the heat of the flue gas in this unit transferred to the succeeding units to the total heat output of the unit reduces from 56.1% in the first unit to 25.8% in the third unit. The physical heat of sinter increases from 192.2 kJ in the first unit to 2290.9 kJ in the third unit. The ratio of the physical heat of sinter to the total heat output of the unit increases from 5.68% in the first unit to 49.3% in the third unit.

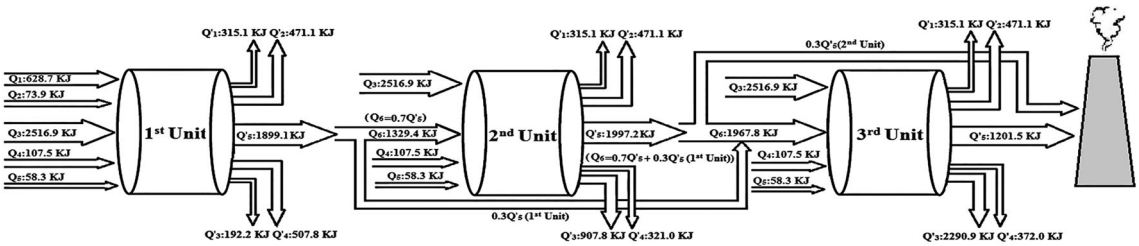

Heat Income	Symbols	Q_1	Q_2	Q_3	Q_4	Q_5	Q_6
	Meaning	The burning of ignition fuel	The physical heat of ignition air	The burning of sintering fuel	The physical heat of sintering mixture	Chemical reaction heat	The heat come from the flue gas in upper unit to the next units
Heat Output	Symbols	Q'_1	Q'_2	Q'_3	Q'_4	Q'_5	/
	Meaning	Evaporation of moisture	The decomposition of carbonates	The physical heat of sinter	Heat loss	The heat of flue gas in this unit transfers to the next units	/

Fig. 4 Heat balance diagram of each calculation unit

Table 2 Accumulation heat ratio and the coke powder addition of each unit

	First unit	Second unit	Third unit
η_{tol} (%)	–	35.30	50.60
η_{avl} (%)	–	33.13	42.31
The coke powder addition to each unit (kg/t)	64.5	55.7	50.8
The coke powder addition ratio in raw materials for each unit (%)	6.6	5.7	5.2

The η_{tol} increases from 35.3% in the second unit to 50.6% in the third unit. The η_{avl} increases from 33.1% in the second unit to 42.3% in the third unit. The coke powder addition of each unit reduces from 64.5 kg/t in the first unit to 50.8 kg/t in the third unit. Its addition, its ratio in raw materials of each unit is 6.6% in the first unit, 5.7% in the second unit, and 5.2% in the third unit.

3.3 Preparation of Raw Materials for Sinter-Pot Test

Based on the above calculation results, the coke powder addition ratio of each part was 6.6%, 5.7%, and 5.2%, respectively. The disk pelletizer was adopted to prepare raw materials. Its main technical parameters included diameter (1000 mm), side height (250 mm), rotational speed (20 r/min), dip (45°), and linear velocity (1.05 m/s). Raw materials preparation process: Firstly, the iron ores and fluxes (including return fines) were mixed uniformly for 2 min in the disk pelletizer and then divided into three equal mass parts. Each part of raw materials with different fuel addition was mixed uniformly and processed into pellets in the disk pelletizer for 3 min. Finally, the three parts of raw materials were put into sinter pot (Fig. 5).

For comparison, the raw materials were prepared simultaneously by conventional method in which all materials were mixed uniformly and then granulated. The raw materials, in which the coke powder addition ratio was 6.6%, were mixed uniformly for 2 min and then granulated for 3 min in the disk pelletizer. The conventional preparation method was called Method A, and the new method was called Method A-1. The sinter produced was defined as Sinter a in which the raw materials were processed by Method A. Sinter a-1 was defined in the same way.

4 Results and Discussion

4.1 The Emission Concentration of SO_2, NO_x, CO, and CO_2 in Sinter-Pot Test

The emission concentration of SO_2, NO_x, CO, and CO_2 of Method A-1 is lower than that of Method A (Fig. 6). Emission of the flue gas can be represented by the integral of its emission concentration-cure over a period of time. Emissions of SO_2, NO_x, CO, and CO_2 of Method A-1 are reduced by 57.7%, 18.4%, 72.5%, and 31.7%, respectively, compared with that of Method A.

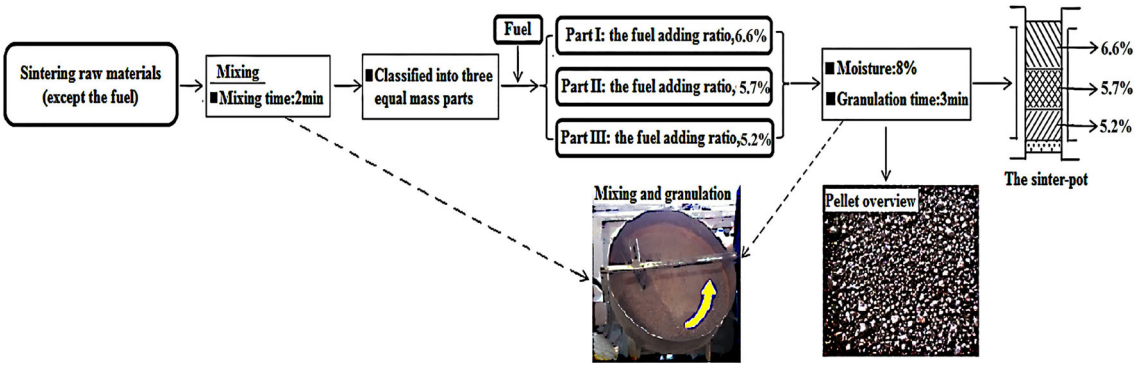

Fig. 5 Preparation process of raw materials of method A-1 (Method A: all materials were mixed uniformly and then granulated)

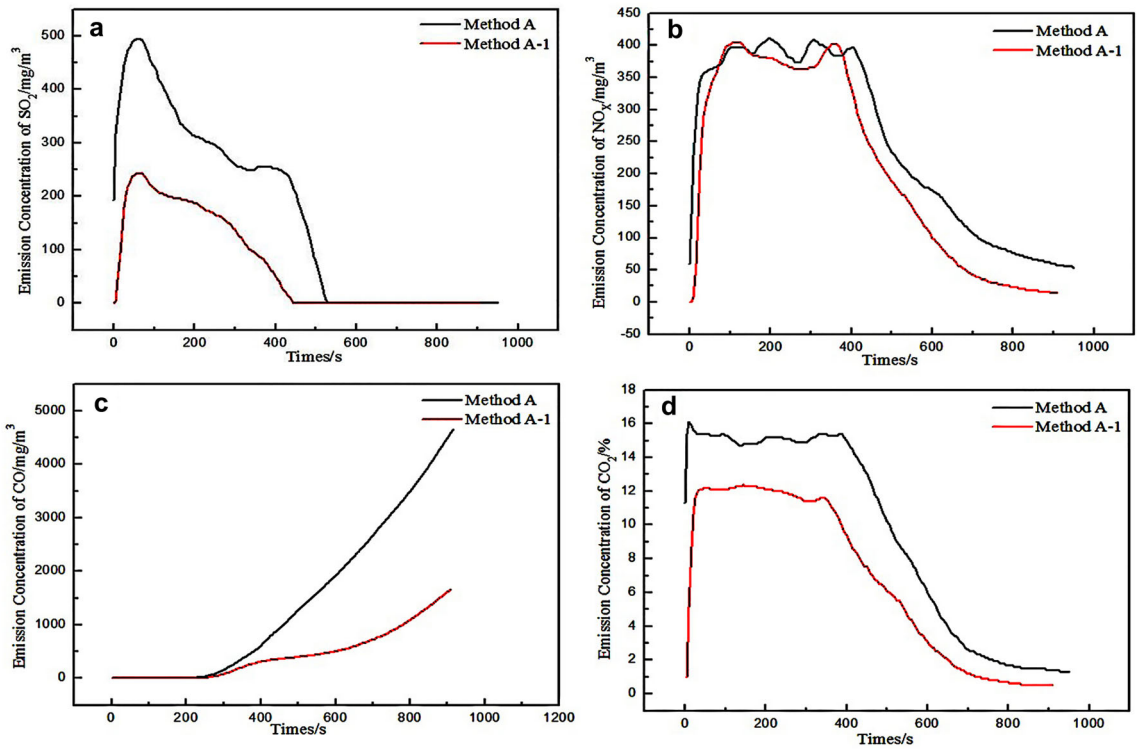

Fig. 6 Emission concentration of SO_2, NO_x, CO, and CO_2 of Method A and Method A-1. **a** SO_2 emission concentration; **b** NO_x emission concentration; **c** CO emission concentration; **d** CO_2 emission concentration

The above results suggest that Method A-1 is helpful to reduce the emissions of SO_2, NO_x, CO, and CO_2 compared with Method A. The main reason is the fuel addition in raw materials is optimized through utilizing the accumulation heat effect of sinter bed. Compared to Method A, in which the coke powder addition ratio is 6.6%, the sinter bed of Method A-1 is divided into three parts, and the coke powder addition ratio of each part of raw materials are 6.6%, 5.7%, and 5.2%, respectively, from the top to the bottom of the pot. The fuel consumption is reduced by 7.5 kg/t. Hence, emission of the iron ore sintering flue gas pollutants get reduced.

4.2 The Sinter Quality

The microstructures and compositions of sinter have significant impact on sinter quality. The content of FeO in Sinter a-1 is less than that in Sinter a (Table 3). The result of FeO content is in agreement with its XRD analysis results (Fig. 7). Meanwhile, the acicular calcium ferrite in Sinter a-1 is more developed than that in Sinter a (Fig. 8). The development of calcium ferrite is advantageous in increasing the sinter strength, and it is also helpful in the reduction reaction of NO_x to N_2 [Eq. (1) and Eq. (2)] [20–22].

Table 3 Chemical compositions of sinter a and sinter a-1 (wt%)

	TFe	FeO	CaO	SiO_2	*S*	*R*
Sinter a	56.2	15.6	10.8	4.91	0.023	2.04
Sinter a-1	56.3	12.2	10.4	4.89	0.032	2.13

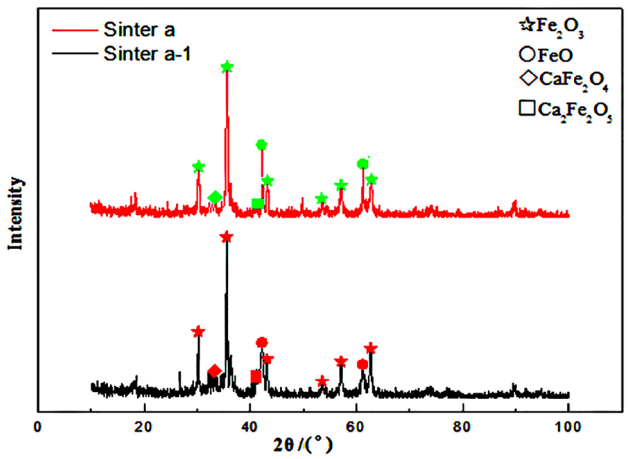

Fig. 7 XRD patterns of Sinter a and Sinter a-1

$$2NO + C \xrightarrow{CF} N_2 + CO_2, \quad (1)$$

$$2NO + 2CO \xrightarrow{CF} N_2 + 2CO_2. \quad (2)$$

Figure 9 shows several major quality indices of sinter. Tumbler strength and RI of Sinter a-1 are higher than those of Sinter a, respectively. The softening–melting properties of sinter are important to the reduction process of the burden and its permeability. In general, it can be evaluated by the characteristic value (*S*, kPa °C) of sinter. The smaller the S value, the better the softening–melting properties of sinter. The *S* value of Sinter a-1 is lower than that of Sinter a, which indicates that the softening–melting properties of Sinter a-1 is better than that of Sinter a.

Previous study have shown that the strength of sinter at room temperature increases with increase in the content of FeO in the sinter [23, 24]. However, it will decrease the sinter strength when FeO content exceedes by 12% in the sinter [25]. The content of FeO in Sinter a and Sinter a-1 are 15.83% and 12.24%, respectively. Meanwhile, the high content of FeO means the generated amount of calcium ferrite is less, and this is obvious in Fig. 8. As a main binding phase of sinter, the decease in calcium ferrite can decrease the sinter strength. This may be the main reason behind the higher strength of Sinter a-1 compared to that of Sinter a.

The content of hematite (Fe_2O_3) and calcium ferrite ($Ca_2Fe_2O_5$, $CaFe_2O_4$, etc.) will increase with the decrease in FeO content in sinter. The hematite and calcium ferrite can be reduced relatively easily. The reduction rates of hematite (Fe_2O_3 49.9%) and calcium ferrite ($Ca_2Fe_2O_5$ 49.9%, $CaFe_2O_4$ 40.1%) are higher than those of other materials in sinter (e.g., Fe_3O_4 26.7%) [25]. It indicates that decreasing FeO content is advantageous to the RI of sinter.

The melting points of Fe_2O_3 (1536 °C), $Ca_2Fe_2O_5$ (1436 °C), and $CaFe_2O_4$ (1216 °C) are higher than that of other materials [25]. As noted above, the content of hematite and calcium ferrite will increase with the decrease in FeO content in sinter. Sinter a-1 has less FeO, the contents of hematite and calcium ferrite in Sinter a-1 are

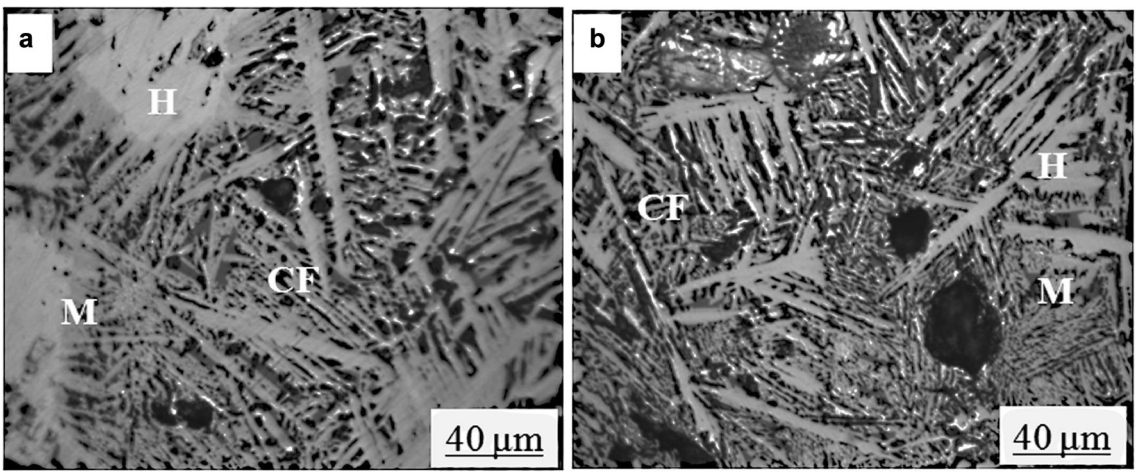

Fig. 8 Optical microstructures of Sinter a (**a**) and Sinter a-1 (**b**). H—Hematite; M—magnetite; CF—calcium ferrite

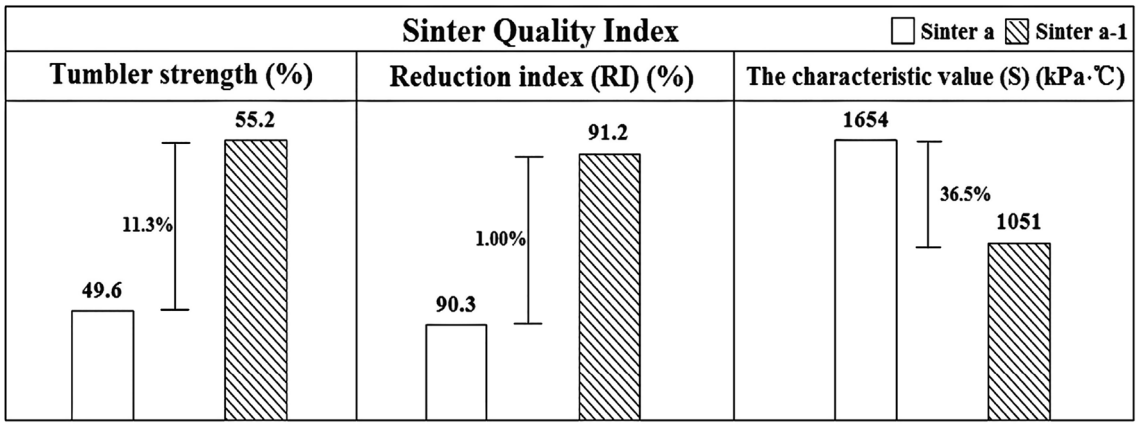

Fig. 9 Major quality indices of Sinter a and Sinter a-1

Table 4 Comparison of Method A and Method A-1 of sinter-pot test

Index (%)	Method	
	A	A-1
Fuel consumption reduction (kg/t)	0	− 7.5
SO_2 emissions reduction (%)	0	− 57.7
NO_x emissions reduction (%)	0	− 18.4
CO emissions reduction (%)	0	− 72.5
CO_2 emissions reduction (%)	0	− 31.7
Tumbler strength change (%)	0	11.3
RI change (%)	0	1.00
S change (%)	0	− 36.5

higher than that in Sinter a. This leads to higher viscosity and reduced mobility of primary slag of Sinter a-1. Hence it becomes more difficult to drop off in the test when compared to that of Sinter a. Meanwhile, the maximum pressure difference of the burden (ΔP_m) and the droplet temperature range (ΔT_2) of Sinter a-1 will be lower than that of Sinter a. According to the expression of the *S*, $S = (\Delta P_m - 0.49) \times \Delta T_2$, the lower ΔP_m and ΔT_2 correspond to lower *S*.

4.3 Comparison of Method A and Method A-1 of Sinter-Pot Test

Method A-1 is preferable compared with Method A from the perspective of reduction in fuel consumption, reduction in emission of SO_2, NO_x, CO, and CO_2, and the improvement in sinter quality (Table 4). It indicates that the reasonable distribution of fuel in sinter bed can not only improve sinter quality, but also reduce the emission of the iron ore sintering flue gas pollutants.

5 Conclusions

From the perspective of reducing the emission of the iron ore sintering flue gas pollutants and making use of the accumulation heat effect of sinter bed, the reasonable distribution of fuel in sinter bed was identified through the calculation of material balance and heat balance of raw materials. The emissions of the iron ore sintering flue gas pollutants were reduced due to the reduction in the fuel consumption in iron ore sintering process. The following conclusions are obtained:

(1) The accumulation heat effect increased gradually from the top to the bottom of sinter-pot. The η_{avl} increased from 33.1% in the second unit to 42.3% in the third unit through the calculation of the accumulation heat effect of sinter bed with a height of 300 mm. The coke powder addition to each unit reduced gradually, and its addition ratios in the raw materials of each unit were 6.6% in the first unit, 5.7% in the second unit and 5.2% in the third unit.

(2) The fuel consumption was reduced by 7.5 kg/t, and the emission of SO_2, NO_x, CO, and CO_2 were reduced by 57.7%, 18.4%, 72.5%, and 31.7%, respectively, compared to the conventional method where the coke powder addition ratio in raw materials was 6.6%. Meanwhile, the sinter quality was improved.

(3) The reasonable distribution of fuel in sinter bed could be realized through reasonable utilization of the accumulation heat effect of sinter bed. Not only did it help to reduce the fuel consumption and improve the sinter quality, but it also helped to reduce the emissions of the iron ore sintering flue gas pollutants.

Acknowledgements This work was supported by the National Key Research and Development Program of China under Grant No. 2017YFB0304001; National Key Research and Development

Program of China under Grant No. 2017YFB0304301; National Natural Science Foundation of China under Grant No. 51234003.

References

1. Hu C Q, and Zhang C X, *J Chin Rare Earth Soc* **22** (2004) 588 (in Chinese).
2. Xu B, Ph D Thesis (2011) (in Chinese).
3. Pan J, Zhu D Q, Xue Z X, Chun T J, and Ruan Z Y, *Environ Chem* **32** (2013) 1660 (in Chinese).
4. Jin Y L, *Sinter Pellet* **29** (2004) 6 (in Chinese).
5. Zhao C L, Wu T, Bo X, and Su Y, *Environ Eng* **32** (2014) 76 (in Chinese).
6. Zhao R Z, and Liang B R, *The Desulphurization and Denitrification Technological Status of Sintering Flue Gases*, in Proc of 2013 national sintering flue gas pollutants integrated treatment technology forum, The Chinese Society for Metals, Datong (2013) (in Chinese).
7. Liu H Q, Fu J X, Liu S Y, Xie X Y, and Yang X Y, *Iron Steel* **51** (2016) 74 (in Chinese).
8. Jiang T, *Sintering and Pelletizing Productive and Technical Manual*, Metallurgical Industry Press, Beijing (2014), p 92 (in Chinese).
9. Zhang J H, Xu N P, and Xie A G, *Energy Metall Ind* **21** (2002) 25 (in Chinese).
10. Song G L, Fu Z H, and Zhang Q, *J Iron Steel Res* **12** (2000) 61 (in Chinese).
11. Kpchko A K, *Cmaib* **1** (1979) 245 (in Russian).
12. Huang Z C, Jiang Y, Mao X M, Xu B, Guo Y F, and Jiang T, *J Cenral South Univ (Sci Technol)* **37** (2006) 884 (in Chinese).
13. Bai C G, Xie X, Qiu G B, Lv X W, Xu G, and Pu X D, *J Chongqing Univ* **31** (2008) 1002 (in Chinese).
14. Masaaki N, Kanji T, and Yoshiyuki M, *ISIJ Int* **55** (2015) 7.
15. Li F S, Zhang X J, Zhang J Y, and Tian W Y, *J Central South Univ (Sci Technol)* **46** (2015) 386 (in Chinese).
16. Zhang B, Zhou J M, and Li M, *J CIESC* **68** (2017) 1811 (in Chinese).
17. Huang X X, Fan X H, Chen X L, Zhao X Z, and Gan M, *Ironmak Steelmak* **2** (2018) 1.
18. Fu J Y, Jiang T, and Zhu D Q, *Sintering and Pelletizing*, Central South University of Technology Press, Changsha (1996), p 105 (in Chinese).
19. Miyer K, *The Research of Iron Ore Spheric Agglomeration*, Metallurgical Technology Press, Beijing (1980), p 112 (in Chinese).
20. Kasai E, Wu S, Sugiyama T, Inaba S, and Omori Y, *Testo-to-Hagané* **78** (1992) 51 (in Japanese).
21. Wu S, Sugiyama T, Morioka K, Kasai E, and Omori Y, *Testo-to-Hagané* **80** (1994) 276 (in Japanese).
22. Kasai E, and Saito F, *Kagaku Kogaku Ronbunshu* **20** (1994) 857 (in Japanese).
23. Umadevi T, Karthik P, Mahapatra P C, Prabhu M, and Ranjan M, *Ironmak Steelmak* **39** (2013) 180.
24. Mochón J, Cores A, Ruizbustinza Í, Verdeja L F, Robla J I, and Garciacarcedo F, *Dyna* **81** (2014) 168.
25. Xu H F, *Sinter Production*, Chemical Industry Press, Beijng (2013), p 242 (in Chinese).